JGP Journal of General Physiology

HYPOTHESIS

Ion channels can be allosterically regulated by membrane domains near a de-mixing critical point

Ofer Kimchi[1,2], Sarah L. Veatch[3], and Benjamin B. Machta[1,4,5,6]

Ion channels are embedded in the plasma membrane, a compositionally diverse two-dimensional liquid that has the potential to exert profound influence on their function. Recent experiments suggest that this membrane is poised close to an Ising critical point, below which cell-derived plasma membrane vesicles phase separate into coexisting liquid phases. Related critical points have long been the focus of study in simplified physical systems, but their potential roles in biological function have been underexplored. Here we apply both exact and stochastic techniques to the lattice Ising model to study several ramifications of proximity to criticality for idealized lattice channels, whose function is coupled through boundary interactions to critical fluctuations of membrane composition. Because of diverging susceptibilities of system properties to thermodynamic parameters near a critical point, such a lattice channel's activity becomes strongly influenced by perturbations that affect the critical temperature of the underlying Ising model. In addition, its kinetics acquire a range of time scales from its surrounding membrane, naturally leading to non-Markovian dynamics. Our model may help to unify existing experimental results relating the effects of small-molecule perturbations on membrane properties and ion channel function. We also suggest ways in which the role of this mechanism in regulating real ion channels and other membrane-bound proteins could be tested in the future.

Introduction

In addition to separating the cell from its surroundings, the plasma membrane is home to diverse functional processes. Membrane-bound ion channels sense chemical and electrical signals and control conductance to specific ions, leading to the complex dynamics that underlie neural function. Although most ion channels are broadly classified as ligand gated or voltage gated, many are also sensitive to a wide range of modulators including calcium levels, pH, temperature, and lipids (Kinnunen, 1991). Ion channel function can depend on the 2-D solvent properties of the membrane in which they are embedded, in both reconstituted (Bristow and Martin, 1987; Rankin et al., 1997) and in vivo assays (Sooksawate and Simmonds, 2001; Allen et al., 2007). Furthermore, structural studies have demonstrated close association between particular lipids and ion channels (Barrantes, 2004; Zhu et al., 2018), sometimes dependent on their functional state (Gao et al., 2016).

Although early efforts assumed the membrane to be a homogenous 2-D solvent for embedded proteins, it is now thought that the membrane is heterogeneous, with liquid structures often termed "rafts" at length scales of 10–100 nm, much larger than the 1-nm scale of individual lipids (Simons and Toomre, 2000; Dart, 2010). Neurotransmitter receptors are often found to be associated with ordered membrane domains when probed with biochemical methods (Allen et al., 2007), sometimes in a subtype-specific manner (Li et al., 2007). Many channels and channel scaffolding elements are posttranslationally lipidated with palmitoyl groups (Fukata and Fukata, 2010; Fukata et al., 2013; Borroni et al., 2016; Globa and Bamji, 2017), and mutation of palmitoylated cysteines reduces their localization to synapses (Christopherson et al., 2003; Rathenberg et al., 2004; Delint-Ramirez et al., 2011). Protein palmitoylation is highly correlated with partitioning into ordered membrane domains in both intact and isolated biological membranes (Levental et al., 2010; Lorent et al., 2018).

Experiments have suggested a physical mechanism that may underlie these structures. Vesicles isolated from mammalian cell lines have membranes tuned close to a liquid–liquid miscibility critical point (Veatch et al., 2008). When cooled below their critical temperature, T_c, these vesicles macroscopically phase separate into two liquid phases termed liquid ordered (l_o) and liquid disordered (l_d), which differ in the partitioning of lipids, proteins, and a fluorescent dye (Baumgart et al., 2007). Experiments

[1]Department of Physics, Princeton University, Princeton, NJ; [2]Harvard Graduate Program in Biophysics, Harvard University, Cambridge, MA; [3]Department of Biophysics, University of Michigan, Ann Arbor, MI; [4]Lewis-Sigler Institute, Princeton University, Princeton, NJ; [5]Department of Physics, Yale University, New Haven, CT; [6]Systems Biology Institute, Yale University, West Haven, CT.

Correspondence to Benjamin B. Machta: benjamin.machta@yale.edu.

suggest that in physiological conditions, plasma membranes exist close to but above a miscibility criticality point. In this nearly critical region, they are expected to display a range of critical phenomena that arise because the free energy cost of making relatively large domains becomes comparable to the thermal energy. Components of a fluid membrane are expected to exhibit long-range correlations in space, with a correlation length ξ that diverges as the critical point is approached, $\xi \sim (T - T_c)^{-\nu}$ (Cardy, 1996). Critical systems also have a long memory, with a correlation time τ that diverges as the critical point is approached, $\tau \sim \xi^z$ with z a dynamic critical exponent (Hohenberg and Halperin, 1977; Honerkamp-Smith et al., 2012). In addition, changing control parameters such as temperature and the addition of small molecules to the chemical environment leads to large changes to system properties. The influence of a small change in system parameters on physical properties ("susceptibility") diverges as the critical point is approached, leaving membrane properties particularly sensitive to external perturbations in their critical region. Systems near criticality exhibit "universal" properties that are largely independent of the microscopic properties of the particular system under consideration, making them highly amenable to quantitative description with highly simplified models, a property we take advantage of here.

Previously, we have argued that proximity to this critical point is likely to underlie much of the raft heterogeneity seen in diverse membrane systems (Machta et al., 2011), with embedded proteins subject to long-range critical Casimir forces (Machta et al., 2012). More recently, we have shown that n-alcohol anesthetics take membrane-derived vesicles away from criticality by lowering T_c (Gray et al., 2013). Despite structural diversity, n-alcohol anesthetics are known to exert similar effects on diverse ion channels (Franks and Lieb, 1994), leading us to speculate that these effects might arise because anesthetics mimic or interfere with native regulation of channels by their surrounding membrane. In support of this, we found that several conditions that reverse anesthetic effects on ion channels and organisms also raise critical temperatures in vesicles (Machta et al., 2016).

In this study, we explore several consequences of thermodynamic criticality for a membrane-bound protein whose internal state is coupled to the state of its surrounding membrane. This study is motivated in part by the observation that many hydrophobic compounds exert influence both on the critical temperature of membrane de-mixing and on ion channel function. Although some of these compounds likely interact directly with hydrophobic regions of ion channels (Mihic et al., 1997; Borghese et al., 2006; Nury et al., 2011; LeBard et al., 2012; Yip et al., 2013), this work focuses on what influence they could have indirectly, through their effects on membrane thermodynamics.

We develop a simple model for an ion channel regulated by its surrounding membrane by coupling a lattice Ising model of a membrane to a highly abstracted lattice ion channel. We show that when the membrane is held close to a critical point, this type of coupling leads to a qualitatively distinct regime including strong responses to perturbations that influence T_c, a hierarchy of time scales, and non-Markovian dynamics. Additionally, we show that these effects are critical phenomena, arising from the diverging generalized susceptibilities and correlation times that emerge near the critical point. This demonstrates that the effects we observe arise not from details inherent to our model, but from the proximity to a critical de-mixing transition. Even though our model is a drastic simplification of real membrane/protein systems, the conclusions drawn are expected to be relevant to these systems when membranes exhibit critical behavior and when proteins exhibit multiple functional states with altered domain affinity.

Materials and methods

Two classes of computer simulations are used in this manuscript, each simulating a 2-D lattice Ising model decorated with a single lattice channel as described in Results. For measurements of mean conductance, we made use of a recently developed algorithm that deterministically computes exact free energies for 2-D lattice spin models (Thomas and Middleton, 2013) with user-specified numerical precision. All results presented from this algorithm were computed on 128 × 128 lattices using 1,028-bit numbers. Lattice parameters and lattice channel boundary conditions were determined as described in Results and Discussion. Couplings between sites that are plus or minus infinity are set to ±10 in our implementation because computations become very slow when couplings are larger and because this leads to acceptably small errors. We expect errors of order e^{-20}, corresponding to the ratio of Boltzmann factors between correct and incorrect couplings. For dynamic simulations, we used the Kawasaki algorithm, a Markov-chain Monte Carlo procedure whose dynamics are in the model B universality class (Hohenberg and Halperin, 1977). All dynamic simulations were performed on 128 × 128 lattices with temperature and lattice channel boundary conditions as described in Results. We define a sweep to be a time step in which 128^2 moves are attempted, so that every spin is attempted to move on average twice. Every sweep, we supplement these dynamics with a single attempt to flip the lattice channel to satisfy detailed balance according to the Metropolis probability.

Online supplemental material

In the supplemental material, we first provide a more detailed argument for the form of the scaling function needed to capture fixed/free boundary conditions used to make Fig. 2 D. We then discuss the scaling form of the dynamic correlation function $\chi(\tau,r,\xi)$ and the effect of our choice of $J_R \to \infty$. Finally, we discuss subtleties in our Gaussian blurring procedure used to make Fig. 3 A. Figure S1 shows that results are robust to changes in J_R. Figure S2 shows results are robust to resolution of Gaussian blurring.

Results and discussion

We consider a lattice system consisting of membrane degrees of freedom $\{s\}$ and a single hypothetical lattice channel (Fig. 1 A) with state R and Hamiltonian $\mathcal{H}_{tot}(\{s\},R)$. The Hamiltonian of our combined system comprises three components:

$$\mathcal{H}_{tot}(\{s\},R) = \mathcal{H}_{mem}(\{s\}) + E_R + \mathcal{H}_{int}(\{s\}_\partial,R), \quad (1)$$

where $\mathcal{H}_{mem}$ describes interactions of membrane lipids with one another, E_R measures the energy of the lattice channel in

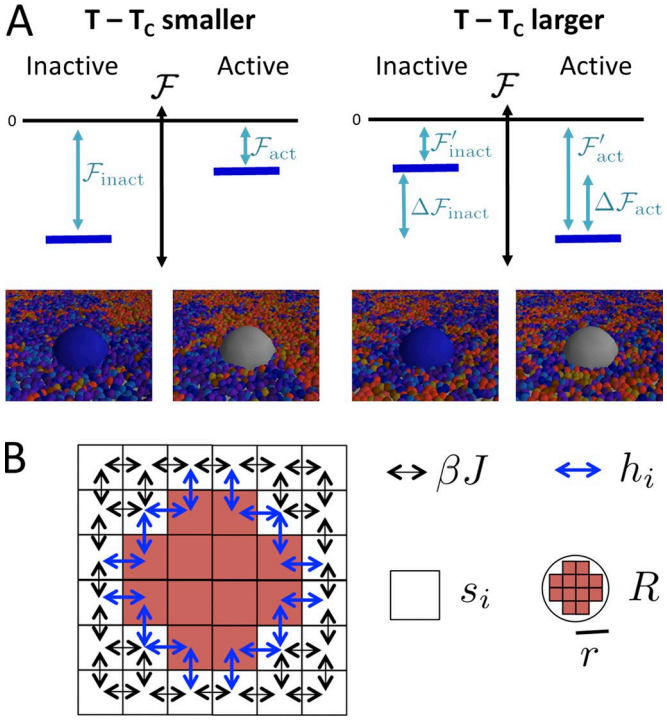

Figure 1. **Schematic representation of our model. (A)** We consider a protein embedded in a nearly critical membrane with which it interacts through distinct boundary interactions in distinct functional states. When the parameters of the membrane change, the free energies of different protein states change, altering function. **(B)** We probe these effects using a lattice Ising model in which a single protein is modeled as a group of sites that transition together, while the remaining membrane is composed of Ising spins that can take values $s_i = \pm 1$.

state R without considering membrane interactions, and $\mathcal{H}_{int}$ describes the interaction between the lattice channel in state R and the components that it contacts at its boundary, which we notate by $s \in \partial$.

As in previous work, we model the membrane as a square lattice of spins $s_1 = \pm 1$ with the usual Ising Hamiltonian

$$\mathcal{H}_{mem} = -J\sum_{i,j} s_i s_j,$$

where the sum runs over all nearest neighbor pairs, neither of which are contained in the lattice channel. In our model, up/down spins roughly correspond to more ordered/disordered domain partitioning components, with a lattice constant corresponding to $l \sim 1$–2 nm of membrane. This scale is based both on the approximate size of a lipid of ~0.8 nm^2 (Chiu et al., 2002; Alwarawrah et al., 2010) and on measurements of the correlation length near the critical point of cell-derived vesicles that suggest an analogy to a lattice model with $l \sim 2$ nm (Veatch et al., 2008). The lattice channel contained in our model has an internal state that can take two values, $R = \pm 1$, which could correspond to open/closed. This state can be affected by a chemical potential (perhaps modulated by a ligand) that in our model contributes a term in the Hamiltonian $E_R = -\mu R$. Crucially, we also include an interaction between membrane and lattice channel of the form

$$\mathcal{H}_{int} = \sum_{i\in\partial} h_i(R) s_i,$$

where this sum is over spins that border the lattice channel, whose boundary conditions in state R are determined by $h_i(R)$ (Fig. 1 B). These interactions between our lattice channel's state R and surrounding spins mimic a coupling between a protein's functional state and the membrane's state as seen experimentally (Bristow and Martin, 1987; Sooksawate and Simmonds, 2001; Allen et al., 2007). They could arise from hydrophobic mismatch (Andersen and Koeppe, 2007; Soubias et al., 2008), distinct lateral pressure profiles in the different phases (Gruner and Shyamsunder, 1991), or specific interactions with particular components that partition strongly into distinct phases (Levitan et al., 2014).

In previous work, we have considered a similar model for a protein's fixed interaction with its surrounding membrane to understand the membrane-mediated critical Casimir forces that act on a pair of proteins (Machta et al., 2012). Previous authors have also considered the role of single-site proteins in an Ising model which are driven out of equilibrium and which thereby prevent phase separation (Sabra and Mouritsen, 1998). To understand how criticality could directly influence protein conformational equilibria, we consider three types of boundary conditions: fixed boundary conditions in which $h_i(R) = \pm J_R$, free boundary conditions in which $h_i(R) = 0$, and Janus boundary conditions in which $h_i(R) = +J_R$ on one side of the lattice channel and $h_i(R) = -J_R$ on the other side. We consider these simplest boundary conditions to gain a qualitative understanding of the effects of different boundary conditions on the lattice channel's static properties. For our studies of mean activity, we use $J_R \to \infty$ for consistency with our past work (Machta et al., 2012), corresponding directly to a physical system in which a lattice channel of slightly larger radius has interaction energy $h_i = J$. In the supplemental text, we explore the dependence of our results on the strength of the coupling J_R. We find that the large interaction energies we use will give quantitatively similar results to a system in which a lattice channel of the same radius has interactions at least on the order of k_BT.

Lattice channel average conductance

We first investigated how a change in the membrane's properties might influence average channel activity, as would be measured by a whole-cell recording or other technique probing the response of many channels together. In our model, the membrane and the lattice channel embedded within it are in thermal equilibrium. Membrane (Ising spin) degrees of freedom are tuned close to a liquid–liquid miscibility critical point, and a single lattice channel interacts with the membrane by preferring different local liquid environments when in different functional states. In equilibrium, the system consisting of lattice channel and membrane will be in a given state with probability determined by an appropriate Boltzmann distribution,

$$P(\{s\},R) = e^{-\beta\mathcal{H}_{tot}(\{s\},R)}/Z,$$

where Z is defined such that the sum of probabilities is unity.

We can integrate over membrane degrees of freedom to isolate the lattice channel whose internal states are occupied according to $P(R) = \exp(-\beta\mathcal{F}_R)/Z$, where

$$\exp(-\beta\mathcal{F}_R) = \sum_{\{s\}} \exp[-\beta\mathcal{H}_{tot}(\{s\},R)] \quad (2)$$

defines $\mathcal{F}_R$, the free energy of state R.

In the context of our model, changes to membrane miscibility influence lattice channel activity if $P(R)$ depends on the details of $\mathcal{H}_{mem}$. Changes to $\mathcal{H}_{mem}$ can lead to a change in a state's free energy $\Delta\mathcal{F}_R$, with resulting changes in $P(R)$. In this two-state example, the membrane influences the activity of the lattice channel, $P(R=\pm1)$, through changes to $\Delta\mathcal{F}_{diff} = \Delta\mathcal{F}_{+1} - \Delta\mathcal{F}_{-1}$. In the case where $P(R=\pm1) \ll 1$, $P(R=+1)$ increases by a factor of $\exp(-\beta\Delta\mathcal{F}_{diff})$. In the general case, the ratio $P(R=+1)/P(R=-1)$ increases by $\exp(-\beta\Delta\mathcal{F}_{diff})$. Thus $\exp(-\beta\Delta\mathcal{F}_{diff})$ measures the degree to which a change in $\mathcal{H}_{mem}$ potentiates the + state (Fig. 2 A).

It is often difficult to estimate free energies from simulation, but for 2-D lattice systems, there has been substantial recent progress (Thomas and Middleton, 2013), which we can use for our lattice membrane/channel system. To study the static properties of our equilibrium system, we make use of a remarkable algorithm developed for spin glasses that uses Pfaffian elimination to exactly calculate partition functions to user-specified precision on lattices with arbitrary nearest neighbor couplings J_{ij} in zero field (Thomas and Middleton, 2013). We implement the Hamiltonian defined previously by setting all interactions J_{ij} between spins to βJ, interactions between lattice sites internal to the lattice channel to minus infinity, and interactions between lattice sites contained in the lattice channel and spins to $h_i(R)$ (Fig. 1 B).

We estimate the potentiation of function that accompanies a 1% change in T_c, comparable both to the natural variation seen in cell-derived vesicles (Veatch et al., 2008) and to the magnitude of the effect seen with physiologically relevant concentrations of n-alcohols (Gray et al., 2013). We examine boundary conditions in which the $R=-1$ state has fixed boundary conditions ($h_i=+\infty$), whereas the $R=+1$ state has either free boundary conditions ($h_i=0$) or Janus boundary conditions. The results are shown in Fig. 2 (B–D). In Fig. 2 B, this potentiation is shown for lattice channels in which the $R=+1$ state has free boundary conditions, at $T=1.05T_c$, for channels with a range of radii (the lattice channels are displayed in Fig. 4 and in the supplemental material, and the radii are calculated as the radius of the circle circumscribing each lattice channel). Larger lattice channels see more pronounced potentiation owing to the increased boundary length of interaction. In Fig. 2 C, the potentiation is shown for the same lattice channels over a range of temperatures. Away from the critical point, this change has only a small effect on the state occupancy—the potentiation is small. However, near the critical point, the potentiation becomes much larger, even for the modest 1% change in T_c explored here. This change in T_c is comparable to that seen with addition of clinically relevant concentrations of anesthetic (Gray et al., 2013; Machta et al., 2016). For the largest lattice channel sizes explored here, our observed potentiation is similar to that observed for the $GABA_A$ channel (see Fig. 2 of Franks and Lieb [1994]) whose radius is ∼6 nm. Although we do not know details of $GABA_A$'s interaction with its surrounding membrane, our results imply that anesthetic effects on membrane T_c could in principle lead to observed changes in channel function even in the absence of direct binding interactions between compound and channel.

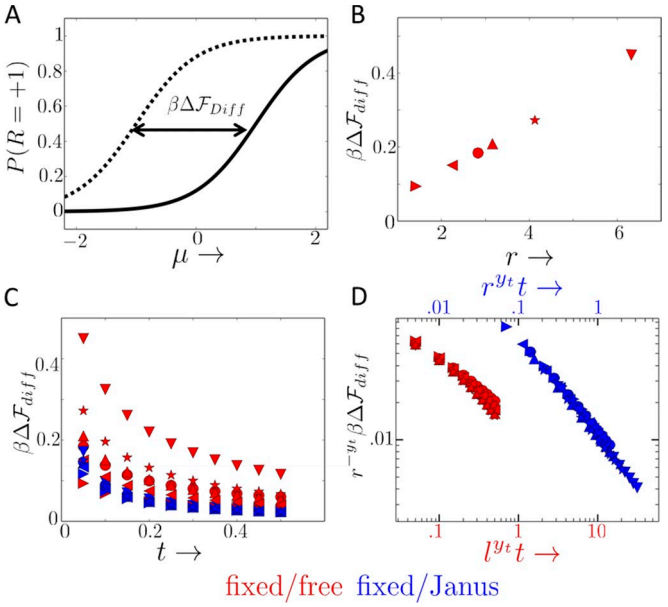

Figure 2. **Changes in membrane properties lead to changes in the conformational equilibrium of a membrane-bound protein. (A)** In this example, $P(R=+1)$ is potentiated by a change in the critical temperature of the membrane. As μ is varied (for example through addition of ligand) the lattice channel transitions from the off ($R=-1$) to on ($R=+1$) state. After a perturbation has been applied that changes T_c, the free energy difference between the $R=\pm1$ states has changed by $\beta\Delta\mathcal{F}_{diff}$, shifting the curve of $P(R=+1)$ versus μ to the left (from the black line to the black dashed line). **(B)** $\beta\Delta\mathcal{F}_{diff}$ is plotted for a perturbation in which T_c is lowered by 1% for lattice channels of different sizes, in all cases from $T=1.05T$ and with fixed boundary conditions when $R=-1$ and free boundary conditions when $R=+1$. $\beta\Delta\mathcal{F}_{diff}$ is larger for larger lattice channels, and is ∼0.5 for the largest lattice channels examined, comparable to the $GABA_A$ channel, which is ∼6 nm across and which is potentiated by ∼50% by analogous treatments (Franks and Lieb, 1994). **(C)** $\beta\Delta\mathcal{F}_{diff}$ is plotted versus $t=(T-T_c)/T_c$ for different-sized lattice channels (symbols as in B) for the same fixed-free boundary conditions (red) and for conditions in which $R=+1$ has Janus boundary conditions (blue). In each case, the magnitude of $\beta\Delta\mathcal{F}_{diff}$ becomes much larger closer to the critical point. **(D)** We verify through the scaling collapse discussed in the text that this effect can be understood as a critical phenomenon. Data are calculated using code detailed in Thomas and Middleton (2013) as described in the text with 1,024-bit floating point numbers.

For channels regulated through this mechanism, we expect that, for a given channel and given boundary conditions, different perturbations should have effects on channel activity predicted solely through that perturbation's influence on T_c. Experimental results on three different channels that respond differently to n-alcohols are consistent with this prediction. In Fig. 3, we plot results from whole-cell channel recordings from Mascia et al. (1996), Nakahiro et al. (1996), and Zuo et al. (2001) for several channels in the presence of n-alcohols plotted against extrapolated ΔT_c as investigated in Gray et al. (2013). As shown in the figure, for any given channel, the effects of these n-alcohols are well predicted by their effect on T_c. Although this collapse of the data is certainly suggestive, future work is needed to exclude a more mundane possibility: that it arises because of a mutual correlation of both assays with the hydrophobicity of different n-alcohols.

An Ising lattice at fixed chemical potential for up spins (not included in our model) has a diverging susceptibility; a small

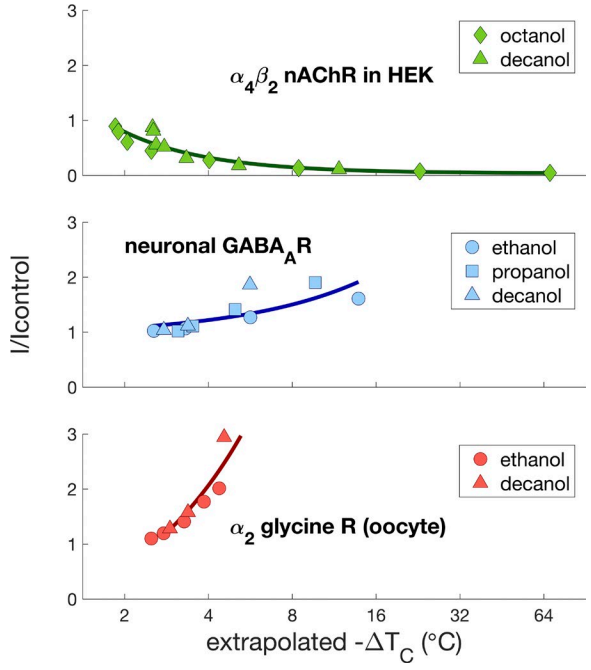

Figure 3. **Whole-cell channel recordings from Mascia et al. (1996), Nakahiro et al. (1996), and Zuo et al. (2001) plotted against extrapolated Δ*Tc* for n-alcohol anesthetics investigated in Gray et al. (2013).** Each channel responds differently to these n-alcohols. However, for each channel, the effects of different n-alcohols can be collapsed on the same curve by rescaling the x axis according to each chemical's efficacy in lowering T_c in cell-derived vesicles.

change in this chemical potential leads to a diverging change in the number of up spins near the critical point, which would result in large changes to the activity of our lattice channel. However, for most components, biological membranes are held at fixed particle number rather than chemical potential, equivalent to fixed number (not chemical potential) of up spins in our model. Changes to the number of up spins, as would accompany biological changes in most lipid levels, do not lead to large changes to the lattice channel's activity. One exception to this could be cholesterol which can be rapidly transferred between internal membranes and the plasma membrane so that its plasma membrane concentration under perturbation is fully described by neither a fixed chemical potential nor a fixed particle number. More broadly, the relationship between particle number and chemical potential requires care to interpret (Ayuyan and Cohen, 2018).

Lattice channel kinetics

We next looked at the role a critical membrane could play in shaping the kinetics of ion channel function as would be measured in single-channel voltage clamp experiments. Real ion channels have kinetics that span a wide array of time scales that are typically understood as arising from internal states of the channel itself (Mortensen and Smart, 2007). Here we consider a hypothetical lattice channel that contains only a single time scale, but that couples to its surrounding lipids, acquiring slower time scales from the critical membrane in which it is embedded. In our studies of dynamics, we consider fixed boundary conditions and use $h_i(R) = RJ$, the same as the interaction between neighboring lipids ($R = \pm 1$ is the state of the lattice channel).

We set $E_R = 0$ to treat both states of the lattice channel symmetrically. We use the local Kawasaki algorithm (Kawasaki, 1972) as we have done previously (Machta et al., 2011) which implements diffusive model B dynamics (Hohenberg and Halperin, 1977). This algorithm exchanges neighboring spins with probabilities chosen to maintain detailed balance. Using these dynamics, a sweep (in which every spin is proposed to exchange with its neighbors once) corresponds to roughly a microsecond of real time, because each lattice site corresponds to the size of a lipid (~1 nm^2) and lipids diffuse at a rate of ~1 μm^2/s (Machta et al., 2011). One caveat is that cells are likely in the regime where hydrodynamic relaxation (Honerkamp-Smith et al., 2012) competes with diffusive dynamics. Our Kawasaki dynamics forbid exchange with spins in the lattice channel, but every sweep the lattice channel changes state with the Metropolis probability to ensure detailed balance.

Although our lattice channel attempts to change its state R during every sweep, its apparent kinetics are much slower. Representative traces of $R(\tau)$ are shown in Fig. 4 A after convolution with a Gaussian of width $\sigma = 10^3$ sweeps. Because patch-clamp recordings measure times on the order of 50–100 μs (Hamill et al., 1981; Kasianowicz et al., 1996; Sakmann and Neher, 2009), we plot $R(\tau)$ after convolution with the Gaussian $k(\tau) = e^{-\tau^2/\sigma^2}$, where $\sigma = 10^3$ (see supplemental material for bare curves and a discussion). Thus, although our lattice channel has only two states, the recording shows short spikes reaching levels in between the two, a feature common to real recordings that presumably has a similar explanation (Hamill et al., 1981). The traces shown in Fig. 4 A share qualitative features with real ion channel traces, spanning many time scales (Mortensen and Smart, 2007): "flickers" shorter than σ, single "openings" (which often contain many short flickers), and "bursts" in which a series of openings occur close to each other. The time scale of these features increases as the critical point is approached (Fig. 4 A). Similar changes in the time scale of ion channel dynamics arising from the addition of some anesthetics have been observed experimentally (Wachtel, 1995). Our findings indicate that these could result from perturbations to the proximity of the membrane to criticality, although they are typically interpreted as arising from direct binding interactions between anesthetic and channel. It is interesting to note that synthetic membranes brought close to a possibly analogous liquid–gel critical point can display currents in the absence of proteins that bear a striking resemblance to those mediated by ion channels (Antonov et al., 1980; Wodzinska et al., 2009). Our results suggest that this commonality may arise because both protein channel and membrane-mediated currents acquire their long time scales from critical fluctuations of the membrane itself.

We quantify these findings by looking at the time autocorrelation of the lattice channel, $\chi(\tau) = \langle R(0)R(\tau)\rangle$ for a range of temperatures (Fig. 4 B), demonstrating that correlations in state persist much longer as the critical point is approached. We also perform simulations for lattice channels of different radii, all at $T = 1.05T_c$ (Fig. 4 C), demonstrating that larger lattice channels have slower kinetics owing to the increased area for interaction

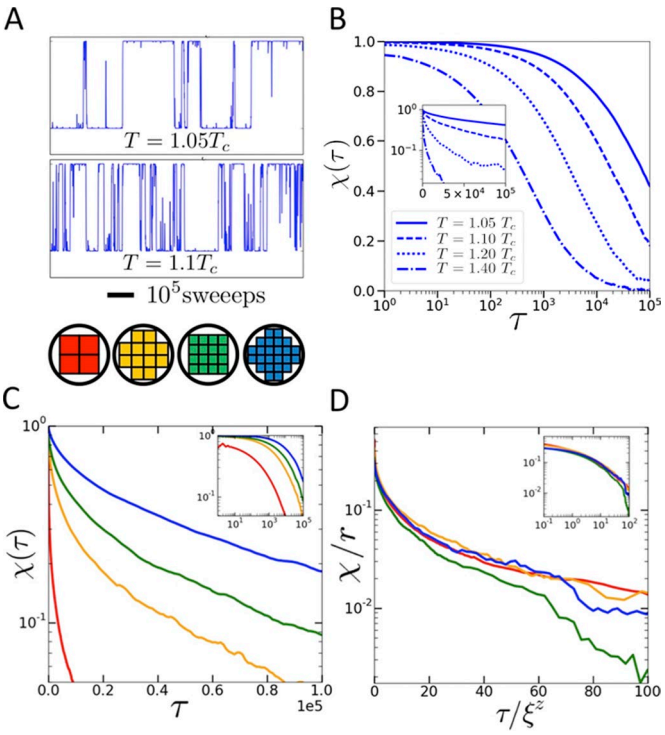

Figure 4. **Lattice channel dynamics acquire slower timescales from the near-critical membrane. (A)** Simulated lattice channel dynamics, $R(\tau)$, have prominent features at many distinct time scales, qualitatively resembling traces from real single-channel recordings (Mortensen and Smart, 2007). Near T_c, lattice channel state changes occur on a time scale orders of magnitude larger than that of attempted state changes, which happen once per sweep. **(B)** The autocorrelation function of $\chi(\tau)$ is shown at different temperatures, with proximity to criticality leading to longer-lived correlations. Deviation of χ from a simple exponential, which would be a straight line in the inset, suggests that protein dynamics occur on many time scales, implying that although the system as a whole is Markovian, the protein considered in isolation is non-Markovian. **(C)** $\chi(\tau)$ also depends on lattice channel radius r at a single temperature, $T = 1.05T_c$ (colors as above). **(D)** These long time scales are critical phenomena. When we plot $\chi(\tau)/r$ versus τ/ξ^z for r and ξ values chosen so that r/ξ is constant, these curves collapse onto a single universal function as predicted by scaling. Each curve is calculated from data from 10^8 sweeps. Simulations were performed on a lattice of $N = 128 \times 128$, and finite size effects were found to be negligible by performing similar studies on lattices of four times the area.

with surrounding membrane. These curves quantify the many time scales that can be seen qualitatively in Fig. 4 A; they are not closely approximated by single exponentials.

Although the combined system of lattice channel and membrane taken together is Markovian, when considered in isolation, the lattice channel displays non-Markovian dynamics, as evidenced by the nonexponential autocorrelation function. This implies that some memory of its history is stored in the membrane degrees of freedom surrounding it. Far from criticality, where no long time scales are inherent to the membrane, this effect is small, and lattice channel kinetics, even when considered in isolation, appear almost Markovian. However, close to the critical point, the lattice channels acquire a range of time scales from the membrane in which they are embedded and have dynamics that are highly non-Markovian. The non-Markovian behavior of several real ion channels and other membrane-embedded proteins has been well characterized, and various internal states of these proteins have been hypothesized (Rankin et al., 1997; Yamashita et al., 2005; Schmauder et al., 2011). It is certainly likely that much of this observed non-Markovian behavior does indeed arise because these channels contain internal states not directly probed with conductance. However, our results suggest that, in some cases, the history of the protein's state may be stored in the membrane rather than in internal states of the protein itself.

Scaling collapse of average conductance

We next wanted to verify that our observed effects could be understood as a critical phenomenon. Properties that arise due to proximity to criticality are often universal, applying to surprisingly diverse real systems as well as simplified minimal models. Scaling functions are a useful tool to probe universality. These functions only describe the universal properties of a system and do not contain the specific details that distinguish different real systems, or even real systems from models within the same universality class. As a result, scaling collapses are important tests of which model predictions are expected to apply to real systems that are qualitatively different in their microscopic details. According to scaling, the free energy associated with inserting a lattice channel with particular boundary conditions should have a universal contribution that depends on lattice channel size, boundary conditions, and the distance to the critical point:

$$\mathcal{F}_R = \mathcal{U}_1(rt^{1/y_t}, h/t^{y_h/y_t}, \ldots), \tag{3}$$

where $y_t = \nu = 1$ and $y_h = \gamma = 15/8$ are the scaling dimension of the fields t and h, r is the radius of the lattice channel, and $\mathcal{U}_1$ is a universal function. Eq. 3 represents our knowledge of the functional form of $\mathcal{F}_R$: although we do not know the specifics of its dependence on t, r, and h, we know from scaling that it does not depend on each independently, but rather on the combinations rt^{1/y_t} and $h/t^{y_h/y_t}$, as well as on other parameters represented by the ellipsis.

Taking a derivative of Eq. 3 with respect to t, we find that

$$\frac{\partial \mathcal{F}_R}{\partial t} = r^{y_t}\mathcal{U}_2(rt^{1/y_t}, h/t^{y_h/y_t}, \ldots), \tag{4}$$

where $\mathcal{U}_2$ is another universal function that is an appropriate sum of derivatives of $\mathcal{U}_1$.

We verify that our measured potentiation can indeed be collapsed in the manner predicted by Eq. 4 in Fig. 2 D for the fixed/Janus boundary conditions. However, for the fixed/free systems, we find an additional contribution that arises more directly from the boundary. This term is proportional to the length of the boundary and should scale as

$$\mathcal{F}_{R,\partial} = r/l\,\mathcal{U}_3(lt^{1/y_t}, h/t^{y_h/y_t}, \ldots), \tag{5}$$

leading to a similar collapse but with $l^{y_t}t$ on the x axis (see supplemental material for discussion). Because the microscopics of our model do not enter into the derivations of the above equations, the collapse to these universal functions depicted in Fig. 2 for our simulations demonstrates that it is the proximity to criticality of our simulations, rather than their microscopic details, that dominate our results.

Scaling collapse of lattice channel kinetics

We expect that the long time scales seen in Fig. 4 A are inherited from the surrounding membrane. Near the Ising critical point, the correlation length diverges as $\xi \propto t^{-\nu}$ (where the rescaled temperature is $t = (T - T_c)/T_c$), and the correlation time diverges as $\tau_{cor} \propto \xi^z$ where a dynamic exponent is $z = 4 - \eta = 3.75$ for the Kawasaki dynamics used here (Hohenberg and Halperin, 1977). If the curves of $R(\tau)$ reflect properties of these slow critical fluctuations, then we might expect that autocorrelation functions in systems with different radii and correlation lengths $\chi(\tau,r,\xi)$ might take a universal form:

$$\chi(\tau,r,\xi) = r^{\lambda}\mathscr{U}(r/\xi,\tau/\xi), \quad (6)$$

with $\lambda = 2y_b = 1$ where y_b is the scaling dimension of the boundary operator, which is expected to be 1/2 from conformal field theory arguments (Cardy, 2004; see supplemental material for a brief discussion). To check this, we performed simulations for the same lattice channels shown in Fig. 4 C but now at different temperatures chosen so that r/ξ is fixed. Although the bare curves decay over time scales that differ by a factor of 10^2, when we plot $\chi(\tau)/r$ versus τ/ξ^z, we see collapse onto a single curve within stochastic error (Fig. 4 D) as predicted by Eq. 6, thus demonstrating that the dynamics observed are critical phenomena.

Conclusions

Regulation by the nearly critical membrane might be very widespread for both ion channels and other membrane-bound proteins. There are hints that the membrane may be playing an important role in localization (Li et al., 2007) and in some cases in direct regulation (Allen et al., 2007) of channels. Our model could account for the sensitivity of many diverse ion channels to chemically diverse anesthetics (Franks and Lieb, 1994), which we have demonstrated lower the critical temperature of cell-derived vesicles by ∼4°K, just over 1% (Gray et al., 2013). Although this model remains to be critically tested, this work suggests that it is thermodynamically feasible for n-alcohols and other hydrophobic components to influence channel function without directly binding to channels. This explanation is appealing in that it might also explain why cholesterol depletion, which changes the membrane's "magnetization" (Zhao et al., 2013), also affects many anesthetic-sensitive channels (Sooksawate and Simmonds, 2001). Recent lipidomics work in neuronal and synaptically derived vesicles have shown that membrane composition undergoes regulated changes during development (Tulodziecka et al., 2016), possibly in part to modulate channel function through a mechanism like the one explored here.

Recent work has demonstrated that anesthetics have little influence on the mean conductance of gramicidin channels, whose gating is quite sensitive to some combination of features of their local membrane environment (Herold et al., 2017). Although those authors interpret this as evidence that anesthetics do not influence membrane properties, our results naturally predict that gramicidin, a small peptide, should be relatively insensitive to changes in T_c. Gramicidin channels dimerize across leaflets, forming a pore and leading to a deformation of the surrounding membrane. The energetic cost of this deformation depends strongly on the hydrophobic thickness of the membrane, leading to dependence of function on some membrane properties. Our work suggests that these relatively small channels would not be particularly sensitive to perturbations that only influence T_c. Perturbations that influence T_c alone do not change the local structure of the membrane dramatically, but instead influence the sizes of typical domains. As such, channels sensitive to T_c must be relatively large. Gramicidin takes up only a slightly larger area than a lipid and is therefore much smaller than anesthetic-sensitive channels, which tend to be ∼10 nm across.

In Weinrich et al. (2017), the authors show that when the membrane is in a single phase state, gramicidin channels have kinetics described by a single exponential for the channel dwell time, consistent with the predictions of our model in the absence of membrane coupling. However, in membranes with two coexisting phases, the channel adopts kinetics that cannot be fitted with a single exponential, but are reasonably well described by a fit to the sum of two exponentials. The authors left open the possibility that the two time scales come from different kinetics in the two phases, or from a mechanism where channels acquired more complex kinetics from switching between the phases. The latter is similar to our model.

Our results suggest that channels modulated in the manner considered here should have their partitioning into small domains modulated by the addition of ligand, a prediction that could be tested using superresolution techniques. In cells, partitioning into larger domains below the critical temperature is likely to be complicated by interactions with the cortical cytoskeleton, which interfere with macroscopic phase separation (Machta et al., 2011). Although macroscopic domains are observed in plasma membrane vesicles isolated from cortical cytoskeleton and viewed at low temperature, it is not known whether these membranes preserve the physical and chemical properties of domains important for channel regulation by this mechanism. Although most previous studies, both by others (Reynwar and Deserno, 2008; Katira et al., 2016) and by ourselves (Machta et al., 2011, 2012), have focused on the role of membrane thermodynamics in localizing proteins into domains, this work suggests that the same domains could couple more directly to function. We predict that when a receptor binds ligand, it will change its preference for its surrounding lipid environment, leading to different interaction partners and an imprint on the state of the local membrane that will persist even after the ligand has dispersed. We have highlighted a specific impact of thermodynamic criticality on a single ion channel, and further work will clarify how this mechanism contributes to neural function.

Acknowledgments

We thank Bill Bialek, Colin Clement, Jim Sethna, and Ned Wingreen for useful discussions. B.B. Machta thanks C.K. Thomas and A.A. Middleton for making their code available on their website.

This work was supported by an National Defense Science and Engineering Graduate Fellowship, National Institute of General Medical Sciences, National Institutes of Health (T32 GM008313 to O. Kimchi and R01 GM110052 to S.L. Veatch), National Science Foundation (MCB 1552439 to S.L. Veatch), and a Lewis-Sigler Fel-

lowship (B.B. Machta). B.B. Machta acknowledges the Aspen Center for Physics and National Science Foundation PHY-1607611.

The authors declare no competing interests.

Author contributions: O. Kimchi, S.L. Veatch, and B.B. Machta designed research, performed research, and wrote the paper.

José D. Faraldo-Gómez served as editor.

Submitted: 10 September 2017
Revised: 24 August 2018
Accepted: 25 October 2018

References

Allen, J.A., R.A. Halverson-Tamboli, and M.M. Rasencik. 2007. Lipid raft microdomains and neurotransmitter signalling. *Nat. Rev. Neurosci.* 8:128–140. https://doi.org/10.1038/nrn2059

Alwarawrah, M., J. Dai, and J. Huang. 2010. A molecular view of the cholesterol condensing effect in DOPC lipid bilayers. *J. Phys. Chem. B.* 114:7516–7523. https://doi.org/10.1021/jp101415g

Andersen, O.S., and R.E. Koeppe II. 2007. Bilayer thickness and membrane protein function: an energetic perspective. *Annu. Rev. Biophys. Biomol. Struct.* 36:107–130. https://doi.org/10.1146/annurev.biophys.36.040306.132643

Antonov, V.F., V.V. Petrov, A.A. Molnar, D.A. Predvoditelev, and A.S. Ivanov. 1980. The appearance of single-ion channels in unmodified lipid bilayer membranes at the phase transition temperature. *Nature.* 283:585–586. https://doi.org/10.1038/283585a0

Ayuyan, A.G., and F.S. Cohen. 2018. Ayuyan and Fredric S. Cohen. The chemical potential of plasma membrane cholesterol: Implications for cell biology. *Biophys. J.* 114:904–918. https://doi.org/10.1016/j.bpj.2017.12.042

Barrantes, F.J. 2004. Structural basis for lipid modulation of nicotinic acetylcholine receptor function. *Brain Res. Brain Res. Rev.* 47:71–95. https://doi.org/10.1016/j.brainresrev.2004.06.008

Baumgart, T., A.T. Hammond, P. Sengupta, S.T. Hess, D.A. Holowka, B.A. Baird, and W.W. Webb. 2007. Large-scale fluid/fluid phase separation of proteins and lipids in giant plasma membrane vesicles. *Proc. Natl. Acad. Sci. USA.* 104:3165–3170. https://doi.org/10.1073/pnas.0611357104

Borghese, C.M., D.F. Werner, N. Topf, N.V. Baron, L.A. Henderson, S.L. Boehm II, Y.A. Blednov, A. Saad, S. Dai, R.A. Pearce, et al. 2006. An isoflurane- and alcohol-insensitive mutant GABA(A) receptor alpha(1) subunit with near-normal apparent affinity for GABA: characterization in heterologous systems and production of knockin mice. *J. Pharmacol. Exp. Ther.* 319:208–218. https://doi.org/10.1124/jpet.106.104406

Borroni, M.V., A.S. Vallés, and F.J. Barrantes. 2016. The lipid habitats of neurotransmitter receptors in brain. *Biochim. Biophys. Acta.* 1858:2662–2670. https://doi.org/10.1016/j.bbamem.2016.07.005

Bristow, D.R., and I.L. Martin. 1987. Solubilisation of the gamma-aminobutyric acid/benzodiazepine receptor from rat cerebellum: optimal preservation of the modulatory responses by natural brain lipids. *J. Neurochem.* 49:1386–1393. https://doi.org/10.1111/j.1471-4159.1987.tb01004.x

Cardy, J. 1996. Scaling and renormalization in statistical physics. Vol. 5. Cambridge, UK: Cambridge University Press. https://doi.org/10.1017/CBO9781316036440

J. Cardy. 2004. Boundary conformal field theory. arXiv:hep-th/0411189v2.

Chiu, S.W., R.E. Jakobsson, J. Mashl, and H.L. Scott. 2002. Cholesterol-induced modifications in lipid bilayers: A simulation study. *Biophys. J.* 83:1842–1853. https://doi.org/10.1016/S0006-3495(02)73949-0

Christopherson, K.S., N.T. Sweeney, S.E. Craven, R. Kang, A.-D. El-Husseini, and D.S. Bredt. 2003. Lipid- and protein-mediated multimerization of PSD-95: implications for receptor clustering and assembly of synaptic protein networks. *J. Cell Sci.* 116:3213–3219. https://doi.org/10.1242/jcs.00617

Dart, C. 2010. Lipid microdomains and the regulation of ion channel function. *J. Physiol.* 588:3169–3178. https://doi.org/10.1113/jphysiol.2010.191585

Delint-Ramirez, I., D. Willoughby, G.R. Hammond, L.J. Ayling, and D.M.F. Cooper. 2011. Palmitoylation targets AKAP79 protein to lipid rafts and promotes its regulation of calcium-sensitive adenylyl cyclase type 8. *J. Biol. Chem.* 286:32962–32975. https://doi.org/10.1074/jbc.M111.243899

Franks, N.P., and W.R. Lieb. 1994. Molecular and cellular mechanisms of general anaesthesia. *Nature.* 367:607–614. https://doi.org/10.1038/367607a0

Fukata, Y., and M. Fukata. 2010. Protein palmitoylation in neuronal development and synaptic plasticity. *Nat. Rev. Neurosci.* 11:161–175. https://doi.org/10.1038/nrn2788

Fukata, Y., A. Dimitrov, G. Boncompain, O. Vielemeyer, F. Perez, and M. Fukata. 2013. Local palmitoylation cycles define activity-regulated postsynaptic subdomains. *J. Cell Biol.* 202:145–161. https://doi.org/10.1083/jcb.201302071

Gao, Y., E. Cao, D. Julius, and Y. Cheng. 2016. Trpv1 structures in nanodiscs reveal mechanisms of ligand and lipid action. *Nature.* 534:347–351. https://doi.org/10.1038/nature17964

Globa, A.K., and S.X. Bamji. 2017. Protein palmitoylation in the development and plasticity of neuronal connections. *Curr. Opin. Neurobiol.* 45:210–220. https://doi.org/10.1016/j.conb.2017.02.016

Gray, E., J. Karslake, B.B. Machta, and S.L. Veatch. 2013. Liquid general anesthetics lower critical temperatures in plasma membrane vesicles. *Biophys. J.* 105:2751–2759. https://doi.org/10.1016/j.bpj.2013.11.005

Gruner, S.M., and E. Shyamsunder. 1991. Is the mechanism of general anesthesia related to lipid membrane spontaneous curvature? *Ann. N. Y. Acad. Sci.* 625(1 Molecular and):685–697. https://doi.org/10.1111/j.1749-6632.1991.tb33902.x

Hamill, O.P., A. Marty, E. Neher, B. Sakmann, and F.J. Sigworth. 1981. Improved patch-clamp techniques for high-resolution current recording from cells and cell-free membrane patches. *Pflugers Arch.* 391:85–100. https://doi.org/10.1007/BF00656997

Herold, K.F., R.L. Sanford, W. Lee, O.S. Andersen, and H.C. Hemmings. 2017. Clinical concentrations of chemically diverse general anesthetics minimally affect lipid bilayer properties. *Proc. Natl. Acad. Sci. USA.* 114:3109–3114. https://doi.org/10.1073/pnas.1611717114

Hohenberg, P., and B. Halperin. 1977. Theory of dynamic critical phenomena. *Rev. Mod. Phys.* 49:435–479. https://doi.org/10.1103/RevModPhys.49.435

Honerkamp-Smith, A.R., B.B. Machta, and S.L. Keller. 2012. Honerkamp-Smith, Benjamin B. Machta, and Sarah L. Keller. Experimental observations of dynamic critical phenomena in a lipid membrane. *Phys. Rev. Lett.* 108:265702. https://doi.org/10.1103/PhysRevLett.108.265702

Kasianowicz, J.J., E. Brandin, D. Branton, and D.W. Deamer. 1996. Characterization of individual polynucleotide molecules using a membranechannel. *Proc. Natl. Acad. Sci. USA.* 93:13770–13773. https://doi.org/10.1073/pnas.93.24.13770

Katira, S., K.K. Mandadapu, S. Vaikuntanathan, B. Smit, and D. Chandler. 2016. Pre-transition effects mediate forces of assembly between transmembrane proteins. *eLife.* 5:e13150. https://doi.org/10.7554/eLife.13150

Kawasaki, K. 1972. Phase transitions and critical phenomena. Vol. 4. Academic Press, Waltham, Massachusetts.

Kinnunen, P.K. 1991. On the principles of functional ordering in biological membranes. *Chem. Phys. Lipids.* 57:375–399. https://doi.org/10.1016/0009-3084(91)90087-R

LeBard, D.N., J. Hénin, R.G. Eckenhoff, M.L. Klein, and G. Brannigan. 2012. General anesthetics predicted to block the GLIC pore with micromolar affinity. *PLOS Comput. Biol.* 8:e1002532. https://doi.org/10.1371/journal.pcbi.1002532

Levental, I., D. Lingwood, M. Grzybek, Ü. Coskun, and K. Simons. 2010. Palmitoylation regulates raft affinity for the majority of integral raft proteins. *Proc. Natl. Acad. Sci. USA.* 107:22050–22054. https://doi.org/10.1073/pnas.1016184107

Levitan, I., K.D. Singh, and A. Rosenhouse-Dantsker. 2014. Cholesterol binding to ion channels. *Front. Physiol.* 5:65. https://doi.org/10.3389/fphys.2014.00065

Li, X., R.D. Serwanski, C.P. Miralles, B.A. Bahr, and A.L. De Blas. 2007. Two pools of triton x-100-insoluble gabaa receptors are present in the brain, one associated to lipid rafts and another one to the post-synaptic gabaergic complex. *J. Neurochem.* 102:1329–1345. https://doi.org/10.1111/j.1471-4159.2007.04635.x

Lorent, J., B.B. Diaz-Rohrer, X. Lin, A. Gorfe, K.R. Levental, and I. Levental. 2018. Structural determinants and functional consequences of protein association with membrane domains. *Biophys. J.* 114(3, Suppl 1):380a. https://doi.org/10.1016/j.bpj.2017.11.2103

Machta, B.B., S. Papanikolaou, J.P. Sethna, and S.L. Veatch. 2011. Minimal model of plasma membrane heterogeneity requires coupling cortical actin to criticality. *Biophys. J.* 100:1668–1677. https://doi.org/10.1016/j.bpj.2011.02.029

Machta, B.B., S.L. Veatch, and J.P. Sethna. 2012. Critical Casimir forces in cellular membranes. *Phys. Rev. Lett.* 109:138101. https://doi.org/10.1103/PhysRevLett.109.138101

Machta, B.B., E. Gray, M. Nouri, N.L.C. McCarthy, E.M. Gray, A.L. Miller, N.J. Brooks, and S.L. Veatch. 2016. Conditions that stabilize membrane domains also antagonize n-alcohol anesthesia. *Biophys. J.* 111:537–545. https://doi.org/10.1016/j.bpj.2016.06.039

Mascia, M.P., T.K. Machu, and R.A. Harris. 1996. Enhancement of homomeric glycine receptor function by long-chain alcohols and anaesthetics. *Br. J. Pharmacol.* 119:1331–1336. https://doi.org/10.1111/j.1476-5381.1996.tb16042.x

Mihic, S.J., Q. Ye, M.J. Wick, V.V. Koltchine, M.D. Krasowski, S.E. Finn, M.P. Mascia, C.F. Valenzuela, K.K. Hanson, E.P. Greenblatt, et al. 1997. Sites of alcohol and volatile anaesthetic action on GABA(A) and glycine receptors. *Nature.* 389:385–389. https://doi.org/10.1038/38738

Mortensen, M., and T.G. Smart. 2007. Single-channel recording of ligand-gated ion channels. *Nat. Protoc.* 2:2826–2841. https://doi.org/10.1038/nprot.2007.403

Nakahiro, M., O. Arakawa, T. Nishimura, and T. Narahashi. 1996. Potentiation of GABA-induced Cl- current by a series of n-alcohols disappears at a cutoff point of a longer-chain n-alcohol in rat dorsal root ganglion neurons. *Neurosci. Lett.* 205:127–130. https://doi.org/10.1016/0304-3940(96)12397-1

Nury, H., C. Van Renterghem, Y. Weng, A. Tran, M. Baaden, V. Dufresne, J.P. Changeux, J.M. Sonner, M. Delarue, and P.J. Corringer. 2011. X-ray structures of general anaesthetics bound to a pentameric ligand-gated ion channel. *Nature.* 469:428–431. https://doi.org/10.1038/nature09647

Rankin, S.E., G.H. Addona, M.A. Kloczewiak, B. Bugge, and K.W. Miller. 1997. The cholesterol dependence of activation and fast desensitization of the nicotinic acetylcholine receptor. *Biophys. J.* 73:2446–2455. https://doi.org/10.1016/S0006-3495(97)78273-0

Rathenberg, J., J.T. Kittler, and S.J. Moss. 2004. Palmitoylation regulates the clustering and cell surface stability of GABAA receptors. *Mol. Cell. Neurosci.* 26:251–257. https://doi.org/10.1016/j.mcn.2004.01.012

Reynwar, B.J., and M. Deserno. 2008. Membrane composition-mediated protein-protein interactions. *Biointerphases.* 3:FA117–FA124. https://doi.org/10.1116/1.2977492

Sabra, M.C., and O.G. Mouritsen. 1998. Steady-state compartmentalization of lipid membranes by active proteins. *Biophys. J.* 74:745–752. https://doi.org/10.1016/S0006-3495(98)73999-2

Sakmann, B., and E. Neher, editors. 2009. Single-Channel Recording. Springer Science & Business Media, Berlin.

Schmauder, R., D. Kosanic, R. Hovius, and H. Vogel. 2011. Correlated optical and electrical single-molecule measurements reveal conformational diffusion from ligand binding to channel gating in the nicotinic acetylcholine receptor. *ChemBioChem.* 12:2431–2434. https://doi.org/10.1002/cbic.201100302

Simons, K., and D. Toomre. 2000. Lipid rafts and signal transduction. *Nat. Rev. Mol. Cell Biol.* 1:31–39. https://doi.org/10.1038/35036052

Sooksawate, T., and M.A. Simmonds. 2001. Effects of membrane cholesterol on the sensitivity of the GABA(A) receptor to GABA in acutely dissociated rat hippocampal neurones. *Neuropharmacology.* 40:178–184. https://doi.org/10.1016/S0028-3908(00)00159-3

Soubias, O., S.L. Niu, D.C. Mitchell, and K. Gawrisch. 2008. Lipid-rhodopsin hydrophobic mismatch alters rhodopsin helical content. *J. Am. Chem. Soc.* 130:12465–12471. https://doi.org/10.1021/ja803599x

Thomas, C.K., and A.A. Middleton. 2013. Numerically exact correlations and sampling in the two-dimensional Ising spin glass. *Phys. Rev. E Stat. Nonlin. Soft Matter Phys.* 87:043303. https://doi.org/10.1103/PhysRevE.87.043303

Tulodziecka, K., B.B. Diaz-Rohrer, M.M. Farley, R.B. Chan, G. Di Paolo, K.R. Levental, M.N. Waxham, and I. Levental. 2016. Remodeling of the postsynaptic plasma membrane during neural development. Mol. Biol. Cell. 27:3480–3489.

Veatch, S.L., P. Cicuta, P. Sengupta, A. Honerkamp-Smith, D. Holowka, and B. Baird. 2008. Critical fluctuations in plasma membrane vesicles. *ACS Chem. Biol.* 3:287–293. https://doi.org/10.1021/cb800012x

Wachtel, R.E. 1995. Relative potencies of volatile anesthetics in altering the kinetics of ion channels in BC3H1 cells. *J. Pharmacol. Exp. Ther.* 274:1355–1361.

Weinrich, M., D.L. Worcester, and S.M. Bezrukov. 2017. Lipid nanodomains change ion channel function. *Nanoscale.* 9:13291–13297. https://doi.org/10.1039/C7NR03926C

Wodzinska, K., A. Blicher, and T. Heimburg. 2009. The thermodynamics of lipid ion channel formation in the absence and presence of anesthetics. blm experiments and simulations. *Soft Matter.* 5:3319–3330. https://doi.org/10.1039/b909877a

Yamashita, M., T. Mori, K. Nagata, J.Z. Yeh, and T. Narahashi. 2005. Isoflurane modulation of neuronal nicotinic acetylcholine receptors expressed in human embryonic kidney cells. *Anesthesiology.* 102:76–84. https://doi.org/10.1097/00000542-200501000-00015

Yip, G.M., Z.W. Chen, C.J. Edge, E.H. Smith, R. Dickinson, E. Hohenester, R.R. Townsend, K. Fuchs, W. Sieghart, A.S. Evers, and N.P. Franks. 2013. A propofol binding site on mammalian GABAA receptors identified by photolabeling. *Nat. Chem. Biol.* 9:715–720. https://doi.org/10.1038/nchembio.1340

Zhao, J., J. Wu, and S.L. Veatch. 2013. Adhesion stabilizes robust lipid heterogeneity in supercritical membranes at physiological temperature. *Biophys. J.* 104:825–834. https://doi.org/10.1016/j.bpj.2012.12.047

Zhu, S., C.M. Noviello, J. Teng, R.M. Walsh Jr., J.J. Kim, and R.E. Hibbs. 2018. Structure of a human synaptic $GABA_A$ receptor. *Nature.* 559:67–72. https://doi.org/10.1038/s41586-018-0255-3

Zuo, Y., G.L. Aistrup, W. Marszalec, A. Gillespie, L.E. Chavez-Noriega, J.Z. Yeh, and T. Narahashi. 2001. Dual action of n-alcohols on neuronal nicotinic acetylcholine receptors. *Mol Pharmacol*, 60:700–711.